GeoVirtual 2020 September 14-16 Resilience and Innovation

# Factors affecting geomembrane strain from differential settlement

H.M.G. Eldesouky, R.W.I. Brachman & R.K. Rowe
*GeoEngineering Centre at Queen's–RMC-Queen's University, Kingston Ontario, Canada*

ABSTRACT
Geomembranes can be very effective at limiting fluid and gas migration in waste cover applications. Strains in the geomembranes from differential settlement of the underlying waste are of interest. Factors affecting geomembrane strain from differential settlement are examined. In most cases, differential settlements occur from density variations and degradation of the waste underlying material. In cold regions, thawing of near surface waste and soil placed when frozen can also lead to differential settlements. Large-displacement finite-element analysis is used to calculate geomembrane strains induced by differential settlement of the waste. The importance of cover component strength and stiffness, interface friction, and bending strains are presented. Results from the finite-element analysis are compared with existing methods to give design engineers new insight into geomembrane response in covers.

RÉSUMÉ
Les géomembranes sont efficaces à limiter de la migration des fluides et gaz dans les applications de reportage de déchet. La déformation de les géomembranes, le résultat de tassement différentiel de la ordures sous-jacent, sont d'intérêt. Des facteurs qui affectent la déformation des géomembranes à cause du tassement différentiel sont examinés. L'importance de la solidité et rigidité du sol et déchets, friction interface et déformation de flexion sont présentés. Les résultats de l'analyse des éléments finis sont comparés avec les méthodes existantes, avec l'intention de donner aux ingénieurs une connaissance approfondie au sujet de la réponse des géomembranes.

## 1 INTRODUCTION

To minimize the migration of contaminated water (and in some cases gases) generated from water percolating through municipal solid waste and mine waste, it is necessary to cover the waste (Rowe et al. 2004). An intact geomembrane is an excellent barrier to most liquids and gases and as a consequence, it is an important element in many cover (a.k.a. cap) designs for waste facilities. However, uneven, or differential, settlement of the waste (Figure 1a), triggered by waste degradation or thawing of frozen waste, induces strain in the geomembrane cover, increasing its vulnerability to rupture and loss of its function as a gas and fluid barrier.

Evaluation of the performance of geomembrane cover, by calculating its strains, should be an essential part of effective post-closure management of waste containment facilities. In many cases, geomembrane strain has been calculated based only on its deformed shape (Giroud et al. 1990, Giroud 1995, Tognon et al. 2000, Hornsey and Wishaw 2012, Eldesouky and Brachman 2018, Marcotte and Fleming 2019). Several studies had investigated, and/or modeled, waste settlement (Edil et al. 1990, Warith et al. 1994, Wall and Zeiss 1995, Ling et al. 1998, Celso et al. 2003, Singh et al. 2010, Simões and Catapreta 2013). By aerial photography, Warith et al. (1994) surveyed the cover of the Trail Road Landfill in Ottawa, Ontario and used the force equilibrium method proposed by Giroud et al. (1990) to calculate tensile stress in the geomembrane. Tognon's strain calculation method (Tognon et al. 2000) was adopted by Divya et al. (2012) to calculate the strain in a geomembrane bridging a cavity in a centrifuge model. Tano et al. (2018) strain gauged geosynthetics, including geomembranes, over a 50 cm wide cavity in a physical large scale model, about 2 m long, and measured their strains under overburden pressure.

Despite all the work that has been done, there is a paucity of studies discussing the interaction of different cover components, namely the cover soil, the geomembrane and the waste, on the deduced geomembrane strains. The geomembrane was studied individually in most of deformed shape based strain calculation methods (Giroud et al. 1990, Giroud 1995, Tognon et al. 2000, Hornsey and Wishaw 2012, Eldesouky and Brachman 2018, Marcotte and Fleming 2019) and the waste is assumed to detach from the cover resulting in a cavity which the geomembrane bridge over. These strain calculation methods have assumptions about how the geomembrane deforms to its final shape. For example, Tognon et al. (2000), Hornsey and Wishaw (2012), and Marcotte and Fleming (2019) consider only small displacements and neglect horizontal displacements of the geomembrane.

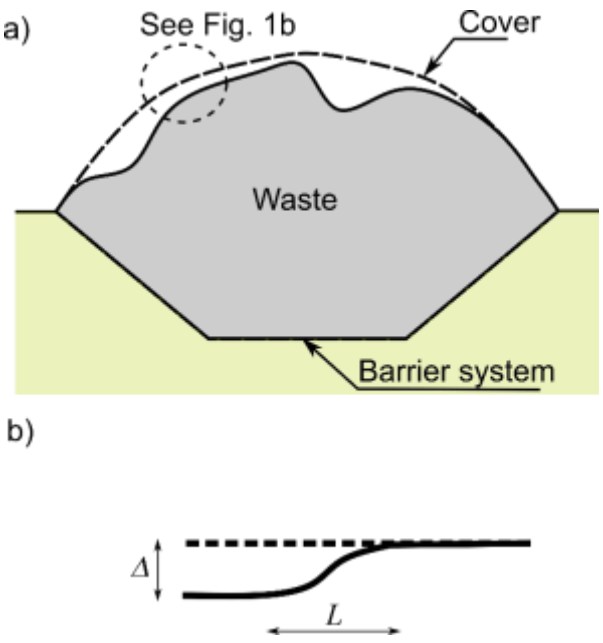


Figure 1. Illustration of differential settlement. a) Initial and deformed shape of the cover, b) geomembrane s-shaped feature at the edge of the settlement zone.

Additionally, the scale of the waste depression, or cavity, studied previously was about one order of magnitude less than real field problem scale. Divya et al. (2012) studied a 30 cm wide cavity while Warith et al. (1994) reported settlement depression width up to 75 m in the Trail Road Landfill. Moreover, Simões and Catapreta (2013) reported a waste settlement up to 1.0 m, about 30% of the waste height, in experimental landfill while Tano et al. (2018) lab model produced 15 cm geomembrane settlement over a 30 cm wide cavity. Also, some of the strain calculation methods used were developed for the gravel indentation problem (Tognon et al. 2000, Hornsey and Wishaw 2012, Eldesouky and Brachman 2018, Marcotte and Fleming 2019) where the deformations are two to three order of magnitude smaller than those associated with cover settlement.

This paper investigates the effect of the interaction between different cover components, each having a different stiffness, on the strain developed in the geomembrane by taking account of the effect of the size of a real waste containment facility, and evaluates the validity of using strain calculation methods that analyze the geomembrane as a discrete unit subject to a prescribed displacement. Finite element analysis was adopted as it: i) can model the geometry of a full scale waste containment facility, ii) takes in account the interaction of different cover components, and iii) allows the calculation of geomembrane strain without any pre-assumed displacement trajectories.

## 2 FINITE ELEMENT ANALYSIS

A waste containment facility with a width of 600 m and top slope of 3% down from the centreline and a maximum waste height of 30 m at the centre was considered by taking the centerline as a line of symmetry for a plane strain half section finite element analysis with smooth-rigid boundary conditions (Figure 2). To allow consideration of differential settlement, as a first approximation, a 100 m wide zone either side of the centreline was assigned a stiffness less than that of the rest of the waste (Figure 2). The waste was assumed to be covered by a 1.5 mm thick linear elastic geomembrane (Young's modulus E = 150 MPa, Poisson's ratio $\upsilon$ = 0.48) overlain by 1 m of cover soil.

The base analysis case parameters and material properties, Table 1, were selected to mimic the behaviour of an idealized waste containment facility. The Young's modulus (E) of the waste was assumed to be 700 kPa for the firmer zone and 400 kPa for the softer zone. These values were inferred from the average settlement strains which ranged from 20-50% (Warith et al. 1994, Wall and Zeiss 1995, Ling et al. 1998) with consolidation and degradation of the waste under an average unit weight of 16 kN/m$^3$ (Rowe et al. 2004) and cover soil with the unit weight of 20 kN/m$^3$. Reported Mohr-Coulomb strength parameters for municipal solid waste (MSW) have a range in apparent cohesion, c, of 0-67 kPa and friction angle, $\phi$, of 23-42° (Table 2). For the base case in this study, the waste was assigned values of c = 25 kPa and $\phi = 25°$. The cover soil properties were selected to simulate a partially desiccated clay, with a negligible cohesion (c = 1 kPa), and a friction angle of $\phi$ = 25°. Upper and lower interface

Table 1. Models parameters used in the analysis

| Case | Interface angle[1] ($\delta_L = \delta_u$) | Cover soil (E = 10 MPa / $\upsilon$ =0.3) | | Waste (E = 700 kPa / $\upsilon$ =0.3) | | Soft zone (E = variable / $\upsilon$ =0.3) | | |
|---|---|---|---|---|---|---|---|---|
| | | c (kPa) | $\phi$ (deg) | c (kPa) | $\phi$ (deg) | E (kPa) | c (kPa) | $\phi$ (deg) |
| 1. Elasto-plastic (base case) | 20° | 1 | 25° | 25 | 25° | 400 | 25 | 25° |
| 2. All-elastic | 20° | - | - | - | - | 400 | - | - |
| 3. Elastic waste | 20° | 1 | 25° | - | - | 400 | - | - |
| 4. Elastic cover | 20° | - | - | 25 | 25° | 400 | 25 | 25° |
| 5. Softer soft zone | 20° | 1 | 25° | 25 | 25° | 350 | 25 | 25° |
| 6. Stiffer soft zone | 20° | 1 | 25° | 25 | 25° | 450 | 25 | 25° |
| 7. Smoother interface | 5° | 1 | 25° | 25 | 25° | 400 | 25 | 25° |

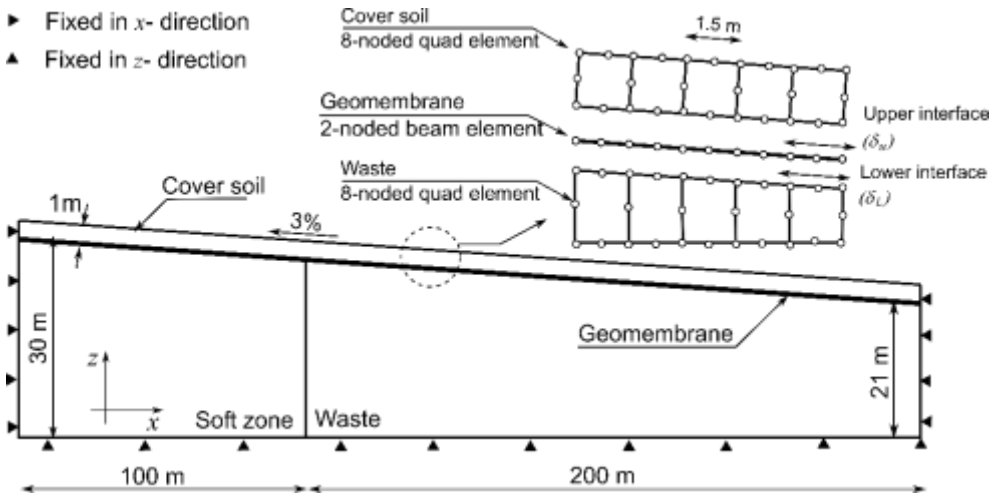


Figure 2. Schematic of the finite element model

Table 2. Mohr-Coulomb shear parameters for waste

| Study | Waste | c (kPa) | ϕ (deg) |
|---|---|---|---|
| Singh et al. (2010) [1] | MSW | 0-67 | 23°-49° |
| Reddy et al. (2009) | MSW | 31-64 | 26°-30° |
| Dixon and Jones (2005)[1] | MSW | 7-24 | 15°-42° |

[1]literature review study

friction angles $\delta_u$ and $\delta_L$, Figure 2, were both taken to be 20° assuming a textured geomembrane.

One aspect of the parametric study considered the effect of the Young's modulus of the softer waste zone from the base case of 400 kPa, by considering the effects of it having E = 350 kPa and 450 kPa (Table 1). The second aspect of the parametric study was modelling the cover soil, waste and/or the soft zone as an elastic material rather than the elasto-plastic model with a Mohr-Coulomb yield surface used in the basic case. The third aspect of the parametric study was to change the two interface friction angles on the base case from 20° to 5° to simulate the effect of using a very smooth geomembrane in the cover (Table 1).

The modelling was conducted using the finite element package ABAQUS (2017). Lagrangian large strain analysis was conducted. Differential settlements were imposed by, first, the own weights were applied on the waste with a uniform and large elastic modulus (E = 6 MPa), resulting in initial stresses. Then the elastic modulus of the various elements was incrementally reduced until the final elastic modulus was achieved. The increments were selected to be sufficiently small to ensure convergence of the solution allowing for both material and geometric nonlinearity.

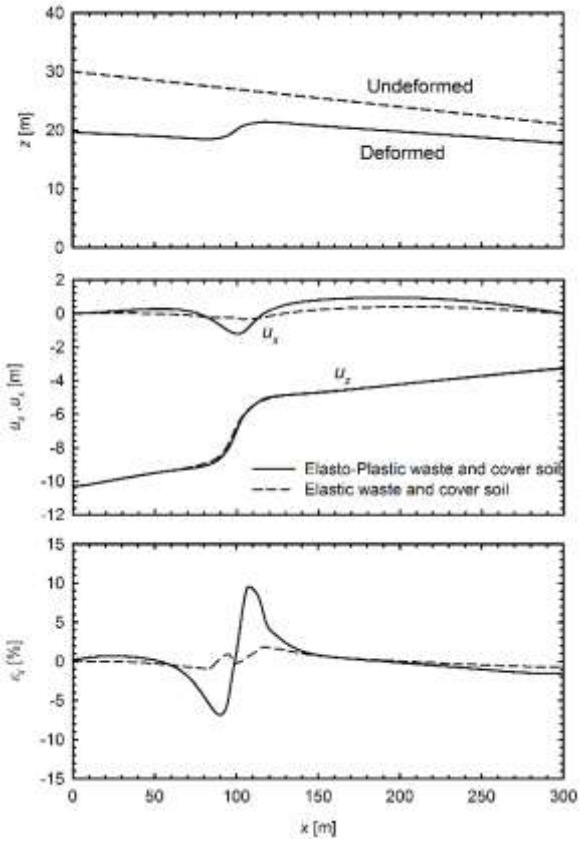


Figure 3. Finite element model results: (a) deformed shape, (b) vertical and horizontal displacements, and (c) inferred geomembrane strain in x-direction.

Table 3. Summary of analysis results

| Model | Slope feature Δ (m) | L (m) | Maximum strain (%) | Bending strain[1] (%) |
|---|---|---|---|---|
| 1. Elastic-plastic | 2.7 | 48.2 | 9.5% | 0.003% |
| 2. All elastic | 2.7 | 48.2 | 1.8% | 0.003% |
| 3. Elastic waste | 2.7 | 48.2 | 7.1% | 0.003% |
| 4. Elastic cover | 2.7 | 48.2 | 1.8% | 0.003% |
| 5. Softer soft zone | 4.0 | 60.0 | 14.5% | 0.006% |
| 6. Stiffer soft zone | 2.4 | 30.3 | 6.2% | 0.001% |
| 7. Very smooth geomembrane | 2.7 | 48.2 | 9.2% | 0.003% |

[1] using Eq. 2

## 3 RESULTS AND DISCUSSION

The elasto-plastic base case (Case 1) gave a maximum settlement (i.e., vertical displacement, $u_z$) of 10.3 m at the centre line of the waste, representing a settlement strain of 34% (Figure 3a and b). At the interface between the soft zone and waste, $x$ = 100 m, the geomembrane formed an s-shaped slope feature (see Figures 1b and 3a) with a depression Δ = 2.7 m over a length L = 48.2 m (Table 3). A maximum geomembrane tensile strain of 9.0% was calculated at the upper curved part of the s- 9.5% was calculated at the upper curved part of the s shape while a minimum strain of -6.8%, i.e. compressive strain, was calculated at the lower curved part (Figure 3c).

All other cases examined, except for those with the softer and stiffer soft zone (Cases 5 & 6), showed insignificant changes in deformed shape, vertical displacement and s-shaped slope feature dimensions, Δ and L (Figure 3 and Table 3). However, the strain calculated in the geomembrane varied significantly, with the maximum strain varying from 1.8% to 9.5% (Table 3). The all-elastic Case 2 (Tables 1 and 3) significantly reduced the maximum strain to 1.8% and changed strain distribution (Figure 3c), with a significant reduction in the horizontal displacement $u_x$, from 1.2 m (Case 1) to 0.3 m (Case 2), Figure 3b.

The model with elastic waste (Case 3) yielded a maximum geomembrane strain of 7.1% while Case 4 with an elastic cover yielded a maximum geomembrane strain of 1.8% similar to the all-elastic model (Table 3). This implies that it is the cover that is controlling the strain in the geomembrane far more than the waste and the cover is assumed to be elastic, and raises the question: why?

In the cases being considered, the geomembrane is embedded between top cover soil above and the waste below and they have opposite strains directions at the same location in the s-shaped slope feature. For example, the waste imposed tensile strains while the cover soil imposed compressive strains on the geomembrane in the upper part of the s-curve and vice versa for the lower part of the s-curve (Figure 4). The resulting final geomembrane strain is dependent on the relative stiffness of the components. In the all-elastic model, the cover soil strain dominates over the waste and soft zone due to its relatively high stiffness, E = 10 MPa for the cover soil compared to 700 and 400 kPa for the waste and soft zone. However, the cover soil stiffness fades in significance in an elasto-plastic analysis due to shear failure that occurs at the induced changes in stress together with the low overburden pressure and low cohesion providing very little shear strength to the cover soil.

The waste settlement increased linearly with the reduction in soft zone elastic modulus (Cases 5, 1, and 6) while the maximum geomembrane strain increased nonlinearly with decreasing soft waste zone stiffness. The reduction of soft zone elastic modulus by one eighth resulted in an increase in the maximum geomembrane strain 1.5-fold from 9.5% (Case 1) to 14.5% (Case 5; Table 3), and the waste settlement at the centre increased by 12% to 11.4 m. The geomembrane maximum strain was reduced to almost two thirds, 6.2% (Case 6) compared to 9.5% (Case 1; Table 3) when the soft zone elastic modulus increased to 450 kPa. The stiffness of the waste and soft zone, and therefore the strain imposed on the geomembrane, changed nonlinearly with elastic modulus due to large displacement and geometric nonlinear nature of the cases analyzed.

In Case 1, the shear stress calculated at the interface between cover components exceeded the interface strength over a small distance of 1.5 m and almost perfect contact was maintained between the modeled cover components and strain was almost fully mobilized between the waste and soft zone and the geomembrane. However, as the interface friction angle was reduced to 5 degrees, more locations slipped and the mobilized strain was slightly reduced, from 9.5% to 9.2%, Table 3.

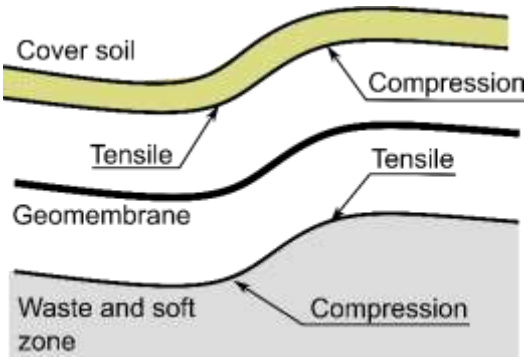


Figure 4. Tensile and compression zones in cover components at the s-shaped feature

## 4 GEOMEMBRANE STRAINS FROM DEFORMED SHAPE

The deformed shape obtained from the finite element analysis was implemented in strain calculation methods (Tognon et al. 2000, Hornsey and Wishaw 2012, Marcotte and Fleming 2019) to asses the applicability of using these methods in strain estimation. The methods,

originally developed for geomembrane liner gravel indentations, assume that the geomembrane only deforms vertically to its deformed shape (Figure 5a). The methods divided the strain into two components; membrane strain $\varepsilon_m$ and bending strains $\varepsilon_b$ except Hornsey and Wishaw (2012) who neglected bending strain. The strain is calculated from the deformed shape $u_z(x)$ and geomembrane thickness t as follows;

$$\varepsilon_m = \sqrt{1 + \left(\frac{\delta u_z}{\delta x}\right)^2} - 1 \quad [1]$$

$$\varepsilon_b = 0.5\, t\, \frac{\delta^2 u_z}{\delta x^2} \quad [2]$$

Eq. 2 yielded a negligible bending strains (Table 3), $\varepsilon_b$ < 0.01%, for the cases analyzed because the geomembrane thickness, in range of mm, was about three order of magnitude less than the curvature (deformed shape second derivative), in range of $m^{-1}$. For the deformations calculated from the elasto-plastic finite element analysis of Case 1, all three methods that neglect deformations in the horizontal plane yielded the same strain with a maximum of 1.6%, 5.9-fold less than the maximum strain calculated by the finite element analysis (Table 3).

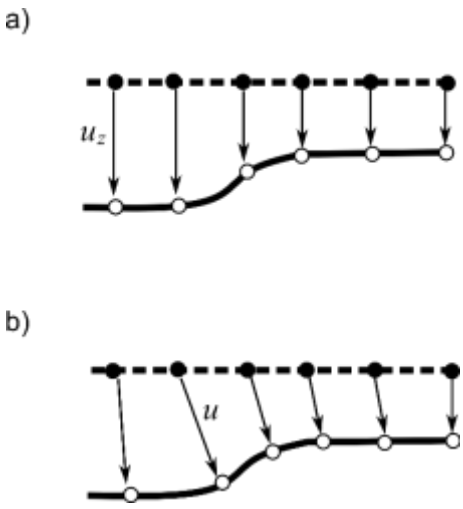


Figure 5. Displacement trajectory for the geomembrane: (a) assuming only vertical displacements ($u_z$), and (b) as inferred from the finite element analysis with vertical and horizontal components of displacement (with resultant u).

The displacement trajectory inferred from the finite element analysis showed the geomembrane deformed both vertically and horizontally (Figure 5b). The horizontal displacement value is dependent on the stiffness of the cover components and changes the strain value greatly. All cases analyzed, except Cases 5 and 6, had essentially identical vertical displacements, and what appears when shown graphically at a natural scale to be the same deformed shape. However, there were significant differences in maximum strain values due to differences in the horizontal displacements which are not easily represented at a natural scale but can give rise to large strains. Thus, the analysis of the deformed shape of these cases using the methods that rely on vertical deformation only to calculate strain yielded the same maximum strain of 1.6%.

## 5 CONCLUSIONS

The effect of the interaction of different cover components on geomembrane strain was investigated using plane strain finite element analysis of a hypothetical waste containment facility. The model dimensions and material parameters were chosen to create an idealized case for the purposes of illustrating the importance of considering the interactions between the components of the system and impact of the resulting horizontal deformations on the calculated strains. The effect of modelling the problem elastically and elasto-plastically has been shown to be significant, with the modelling of the cover soil as an elastic material significantly underestimating the maximum strain. Consideration of the potential for shear failure in the cover soil when it is subjected to large differential settlements would appear critical to the evaluation of strains in the geomembrane. The deformed shape calculated from the finite element analysis was analysed using typical strain calculation methods used for calculating strains due to gravel indentations in a geomembrane and the results were compared with those from the more rigorous finite element analysis. For the cases and materials examined, the following can be concluded:

1. At the edge of the differential settlement depression, the geomembrane forms an s-shaped feature where the maximum strain in the geomembrane develops. The cover soil and waste both developed opposite strain at the same location of the s-shape feature which are imposed on the geomembrane. The final strain imposed on the geomembrane depends on the relative stiffness of the cover soil, waste and soft zone. Low stiffness cover soil, triggered by shear failure, did not impose its strain on the geomembrane, however, the waste and soft zone imposed a maximum strain ranging 7.1% to 9.5% for settlement of 2.7 m over a length of 48.2 m. High stiffness cover, with no shear failure, tended to equalize the strain imposed by the waste and soft zone reducing the maximum calculated strain to 1.8%.
2. The use of a very smooth geomembrane in the cover reduced the maximum strain induced due to its lower interface friction angle. However, attention should be given to cover soil stability if used.
3. A nonlinear relationship was observed between the elastic modulus of the soft zone and the maximum strain. The reduction of soft zone modulus by 12.5% resulted in an increase of maximum strain by 52%,

while increasing it by 12.5% it yielded a maximum strain decrease of almost 35%.

4. Methods of calculating strain based only on the deformed shape vertical displacements can substantially underestimated the maximum strain in the geomembrane.

This study provides first insights into the strains generated in a cover geomembrane by differential settlement and how interactions between the different cover components can effect geomembrane strain. Further study considering less idealized situations is warranted.

## 6 REFERENCES


ABAQUS. 2017. Abaqus/CAE user manual 2017. Dassault Systèmes, Providence, RI, USA.

Celso, A., Marques, M., Filz, G.M., and Vilar, O.M. 2003. Composite Compressibility Model for Municipal Solid Waste. **129**(April): 372–378.

Divya, P. V., Viswanadham, B.V.S., and Gourc, J.P. 2012. Influence of geomembrane on the deformation behaviour of clay-based landfill covers. Geotextiles and Geomembranes, **34**: 158–171. doi:10.1016/j.geotexmem.2012.06.002.

Dixon, N., and Jones, D.R. V. 2005. Engineering properties of municipal solid waste. Geotextiles and Geomembranes, **23**(3): 205–233. doi:10.1016/j.geotexmem.2004.11.002.

Edil, T., Ranguette, V., and Wuellner, W. 1990. Settlement of Municipal Refuse. *In* Geotechnics of Waste Fills—Theory and Practice. ASTM International, 100 Barr Harbor Drive, PO Box C700, West Conshohocken, PA 19428-2959, PO Box C700, West Conshohocken, PA 19428-2959. pp. 225-225–15. doi:10.1520/STP25309S.

Eldesouky, H.M.G., and Brachman, R.W.I. 2018. Calculating local geomembrane strains from a single gravel particle with thin plate theory. Geotextiles and Geomembranes, **46**(1): 101–110. Elsevier. doi:10.1016/j.geotexmem.2017.10.007.

Giroud, J.P. 1995. Determination of Geosynthetic Strain Due to Deflection. Geosynthetics International, **2**(3): 635–641. doi:10.1680/gein.2.0028.

Giroud, J.P., Bonaparte, R., Beech, J.F., and Gross, B.A. 1990. Design of soil layer-geosynthetic systems overlying voids. Geotextiles and Geomembranes, **9**(1): 11–50. doi:10.1016/0266-1144(90)90004-V.

Hornsey, W.P., and Wishaw, D.M. 2012. Development of a methodology for the evaluation of geomembrane strain and relative performance of cushion geotextiles. Geotextiles and Geomembranes, **35**: 87–99. Elsevier Ltd. doi:10.1016/j.geotexmem.2012.05.002.

Ling, H.I., Leshchinsky, D., Mohri, Y., and Kawabata, T. 1998. Estimation of Municipal Solid Waste Landfill Settlement. Journal of Geotechnical and Geoenvironmental Engineering, **124**(1): 21–28. doi:10.1061/(ASCE)1090-0241(1998)124:1(21).

Marcotte, B.A., and Fleming, I.R. 2019. The role of undrained clay soil subgrade properties in controlling deformations in geomembranes. Geotextiles and Geomembranes, **47**(3): 327–335. Elsevier. doi:10.1016/j.geotexmem.2019.02.001.

Reddy, K.R., Hettiarachchi, H., Parakalla, N.S., Gangathulasi, J., and Bogner, J.E. 2009. Geotechnical properties of fresh municipal solid waste at Orchard Hills Landfill, USA. Waste Management, **29**(2): 952–959. Elsevier Ltd. doi:10.1016/j.wasman.2008.05.011.

Rowe, R.K., Quigely, R.M., Brachman, R.W.I., and Booker, J.R. 2004. Barrier Systems for Waste Disposal Facilities. 2nd edition. CRC Press, London. doi:10.1201/9781482271935.

Simões, G.F., and Catapreta, C.A.A. 2013. Monitoring and modeling of long-term settlements of an experimental landfill in Brazil. Waste Management, **33**(2): 420–430. doi:10.1016/j.wasman.2012.10.001.

Singh, M.K., Fleming, I.R., and Sharma, J.S. 2010. Development of a practical method for the estimation of maximum lateral displacement in large landfills. Practice Periodical of Hazardous, Toxic, and Radioactive Waste Management, **14**(1): 37–46. doi:10.1061/(ASCE)1090-025X(2010)14:1(37).

Tano, B.F.G., Stoltz, G., Coulibaly, S.S., Bruhier, J., Dias, D., Olivier, F., and Touze-Foltz, N. 2018. Large-scale tests to assess the efficiency of a geosynthetic reinforcement over a cavity. Geosynthetics International, **25**(2): 242–258. doi:10.1680/jgein.18.00005.

Tognon, A.R., Rowe, R.K., and Moore, I.D. 2000. Geomembrane Strain Observed in Large-Scale Testing of Protection Layers. Journal of Geotechnical and Geoenvironmental Engineering, **126**(12): 1194–1208. doi:10.1061/(ASCE)1090-0241(2000)126:12(1194).

Wall, D.K., and Zeiss, C. 1995. Municipal Landfill Biodegradation and Settlement. Journal of Environmental Engineering, **121**(3): 214–224. doi:10.1061/(ASCE)0733-9372(1995)121:3(214).

Warith, M.A., Smolkin, P.A., and Caldwell, J.G. 1994. Evaluation of an HDPE Geomembrane Landfill Cover Performance. Geosynthetics International, **1**(2): 201–219. doi:10.1680/gein.1.0009.